0026-895X/10/7804-756–766$20.00
MOLECULAR PHARMACOLOGY
Copyright © 2010 The American Society for Pharmacology and Experimental Therapeutics
Mol Pharmacol 78:756–766, 2010

Vol. 78, No. 4
66613/3627994
Printed in U.S.A.

μ-Opioid Receptors: Correlation of Agonist Efficacy for Signalling with Ability to Activate Internalization[S]

Jamie McPherson, Guadalupe Rivero, Myma Baptist, Javier Llorente, Suleiman Al-Sabah,[1] Cornelius Krasel,[2] William L. Dewey, Chris P. Bailey, Elizabeth M. Rosethorne, Steven J. Charlton, Graeme Henderson, and Eamonn Kelly

Department of Physiology and Pharmacology, University of Bristol, Bristol, United Kingdom (J.M., G.R., M.B., J.L., G.H., E.K.); School of Pharmacy, University of Reading, Whiteknights, United Kingdom (S.A., C.K.); Department of Pharmacology and Toxicology, Virginia Commonwealth University Medical Center, Richmond, Virginia (W.L.D.); Department of Pharmacy and Pharmacology, University of Bath, Claverton Down, Bath, United Kingdom (C.P.B.); and Novartis Institutes for Biomedical Research, Horsham, West Sussex, United Kingdom (E.M.R., S.J.C.)

Received May 26, 2010; accepted July 20, 2010

ABSTRACT

We have compared the ability of a number of μ-opioid receptor (MOPr) ligands to activate G proteins with their abilities to induce MOPr phosphorylation, to promote association of arrestin-3 and to cause MOPr internalization. For a model of G protein-coupled receptor (GPCR) activation where all agonists stabilize a single active conformation of the receptor, a close correlation between signaling outputs might be expected. Our results show that overall there is a very good correlation between efficacy for G protein activation and arrestin-3 recruitment, whereas a few agonists, in particular endomorphins 1 and 2, display apparent bias toward arrestin recruitment. The agonist-induced phosphorylation of MOPr at Ser^{375}, considered a key step in MOPr regulation, and agonist-induced internalization of MOPr were each found to correlate well with arrestin-3 recruitment. These data indicate that for the majority of MOPr agonists the ability to induce receptor phosphorylation, arrestin-3 recruitment, and internalization can be predicted from their ability as agonists to activate G proteins. For the prototypic MOPr agonist morphine, its relatively weak ability to induce MOPr internalization can be explained by its low agonist efficacy.

Introduction

Drugs such as morphine that are agonists at the MOPr are of great therapeutic importance in the management of pain and are also highly significant in terms of their abuse potential. MOPr agonists also induce the phenomenon of tolerance whereby increasing doses of the agonist are required to maintain the analgesic or euphoric effect of the drug (Corbett et al., 2006). A number of mechanisms have been proposed to mediate tolerance to opioid agonists (Williams et al., 2001), and in recent years there has been increased focus on the molecular regulation of MOPr as a mechanism of tolerance, in particular with regard to MOPr desensitization and internalization (for reviews, see Connor et al., 2004; Bailey and Connor, 2005; Christie, 2008; Kelly et al., 2008; Koch and Höllt, 2008). Although for some GPCRs there seems to be a clear correlation between agonist efficacy and the ability to induce receptor regulatory processes/mechanisms such as phosphorylation and desensitization, the situation for the MOPr is much less clear, with some evidence indicating that low-efficacy agonists such as morphine are better able to induce tolerance than some higher efficacy agonists (Duttaroy and Yoburn, 1995; Grecksch et al., 2006).

A number of theories have been developed in an attempt to explain these observations (Bailey et al., 2006; Martini and Whistler, 2007; Koch and Höllt, 2008). For example, it has been proposed that MOPr agonists with relatively low efficacy are able to induce profound tolerance because they in-

This work was supported by the Medical Research Council UK [Grant G0600943]; the National Institutes of Health National Institute on Drug Abuse [Grant DA020836]; and the Biotechnology and Biochemical Sciences Research Council [Grant BB/D012902/1].

[1] Current affiliation: Department of Pharmacology and Toxicology, Kuwait University, Safat, Kuwait.

[2] Current affiliation: Department of Pharmacology, School of Pharmacy, Philipps-Universität Marburg, Marburg, Germany.

Article, publication date, and citation information can be found at http://molpharm.aspetjournals.org.

doi:10.1124/mol.110.066613.

[S] The online version of this article (available at http://molpharm.aspetjournals.org) contains supplemental material.

ABBREVIATIONS: MOPr, μ opioid receptor; DAMGO, [D-Ala^2,*N*-$MePhe^4$,Gly-ol]-enkephalin; GPCR, G protein-coupled receptor; HEK, human embryonic kidney; EA, enzyme acceptor; FRET, fluorescence resonance energy transfer; CFP, enhanced cyan fluorescent protein; YFP, enhanced yellow fluorescent protein; HBBS, Hanks' buffered saline solution; ELISA, enzyme-linked immunosorbent assay; M6G, morphine-6-glucuronide; GRK2, G protein-coupled receptor kinase 2; GIRK, G protein-gated K^+ channel; GTPγS, guanosine 5′-*O*-(3-thio)triphosphate.

duce MOPr desensitization but little MOPr internalization such that the receptor is unable to undergo efficient dephosphorylation and resensitization as would occur with a higher efficacy internalizing agonist (Schulz et al., 2004). Alternatively, we have shown that morphine and [D-Ala^2,*N*-MePhe^4,Gly-ol]-enkephalin (DAMGO) induce MOPr desensitization by different molecular mechanisms (Bailey et al., 2006, 2009a,b; Johnson et al., 2006), which could also explain the differing abilities of MOPr agonists to induce or maintain tolerance (Bailey et al., 2006; Hull et al., 2010). A further idea is that the low efficacy of morphine induces little MOPr desensitization and that it is instead the prolonged signaling of the morphine-activated receptor that leads to neuronal adaptations that precipitate tolerance (Whistler et al., 1999). Such ideas have formed the basis of theories of opioid tolerance, such as the relative activity versus endocytosis theory, but these remain the subject of conjecture (see, for example, Martini and Whistler, 2007; Koch and Höllt, 2008).

An important element in the analysis of opioid tolerance is the ability to obtain accurate measurements of agonist efficacy. However, because this property is both a drug- and tissue-dependent quantity, its value for an agonist can vary from tissue to tissue (Christopoulos and El-Fakahany, 1999), which can confound interpretation. For example, some opioid agonists are full agonists in clonal cell lines expressing high levels of MOPr but may be partial agonists in neurons in which MOPr expression is lower and a receptor reserve may not exist (Selley et al., 1998). Perhaps a more useful measure of efficacy is relative intrinsic efficacy (Furchgott and Bursztyn, 1967), which enables comparison of responses produced by equivalent fractional occupancy of the receptors by different agonists in the same tissue. In this case, the tissue factors contributing to efficacy cancel out and the relative intrinsic efficacy thus becomes a measurement of the relative abilities of different agonists to activate the receptor. Operational analysis of agonist responses (Black and Leff, 1983) provides one means of determining the relative intrinsic efficacy of agonists. In this approach, the operational efficacies (τ values) of a series of agonists in a particular cell type or tissue are determined from the concentration-effect data and can be used as a measure of agonist relative intrinsic efficacy (Black and Leff, 1983).

In the present study, we have used operational analysis to determine the τ values of 22 opioid agonists for two signaling outputs of MOPr: G protein activation and nonvisual arrestin recruitment. To achieve this, we have employed high-throughput assay technology to construct full concentration-effect curves for MOPr agonist-induced [^{35}S]GTPγS binding to cell membranes and arrestin-3 recruitment to MOPr in intact cells using the PathHunter assay system. In addition, we have measured the ability of a number of opioid agonists to induce phosphorylation of the MOPr at Ser^{375} and to cause MOPr internalization. Correlation of these measures indicates that for the majority of MOPr agonists there is a good correlation between operational efficacy for G protein activation and activation of the MOPr internalization process.

Materials and Methods

Cell Culture and Transfections. HEK293 cells were maintained at 37°C in 95% O_2, 5% CO_2, in Dulbecco's modified Eagle's medium (Invitrogen, Carlsbad, CA) supplemented with 10% fetal bovine serum, 10 U/ml penicillin, and 10 mg/ml streptomycin. In addition, the culture medium for the HEK293 cells stably expressing T7-tagged MOPr (Bailey et al., 2003; Rodriguez-Martin et al., 2008) contained 250 μg/ml G-418 (Geneticin), a selective antibiotic (PAA, Pasching, Austria).

The PathHunter β-arrestin assay (DiscoveRx Corp., Birmingham, UK) uses enzyme fragment complementation between two portions of β-galactosidase to measure recruitment of β-arrestin to a GPCR after activation. The larger portion, the enzyme acceptor (EA) tag is fused to arrestin-3, and the smaller portion (ProLink) is fused to the C terminus of the GPCR of choice. Activation of the receptor causes recruitment of arrestin-3 to the GPCR, thus forming a functional β-galactosidase enzyme, the activity of which can be measured by the addition of a chemiluminescent substrate. The MOPr:ProLink receptor construct was stably expressed in HEK293 cells stably expressing arrestin-3:EA (DiscoveRx) using Lipofectamine (Invitrogen, Paisley, UK) transfection according to the manufacturer's instructions. Expression was maintained using antibiotic selection (250 μg/ml hygromycin and 500 μg/ml G-418), and cells were passaged at 50% confluence using trypsin/EDTA.

For fluorescence resonance energy transfer (FRET) experiments, the enhanced cyan fluorescent protein (CFP) and enhanced yellow fluorescent protein (YFP) (Clontech, Mountain View, CA) constructs were fused to the COOH terminus of bovine arrestin-3 and the rat MOPr, respectively, as described previously (Krasel et al., 2005). In brief, the stop codon for each protein was replaced with an XbaI site (TCTAGA), and the coding sequences of CFP and YFP were appended in-frame. The pcDNA3-arrestin-3-CFP, pcDNA3-GRK2, and the pcDNA3-MOPr-YFP constructs were verified by sequencing. Transient transfection of HEK293 cells was carried out with Effectene (QIAGEN, Hilden, Germany), if not otherwise indicated, 48 h before use. The ratio between MOPr-YFP DNA and arrestin-3-CFP DNA for transfection was always between 2:1 and 1:1.

[^{35}S]GTPγS Binding Assay. The binding of [^{35}S]GTPγS to membranes prepared from T7-MOPr-expressing cells was based on a protocol described previously (Johnson et al., 2006). Cells were grown to approximately 90% confluence, and removed from the culture flask using a lifting buffer [10 mM HEPES, 0.9% (w/v) NaCl, and 0.2% (w/v) EDTA, pH 7.4] and cell scraper, pelleted by centrifugation (377*g*; 10 min) and resuspended in wash buffer 1 (10 mM HEPES and 10 mM EDTA, pH 7.4). The cell suspension was homogenized with an Ultra-Turrax disperser (five 10-s bursts; IKA-Werke GmbH & Co. KG, Staufen, Germany). The resulting homogenate was ultracentrifuged at 48,000*g* for 30 min at 4°C using an Avanti J-251 ultracentrifuge (Beckman Coulter, Fullerton, CA), the supernatant discarded and the pellet resuspended. This was repeated to wash, and the final pellet resuspended in wash buffer 2 (10 mM HEPES and 0.1 mM EDTA, pH 7.4) at a protein concentration of 3 to 5 mg/ml. Aliquots were flash-frozen and maintained at −80°C until required.

In some experiments, [^{35}S]GTPγS binding was also studied using membranes prepared from the HEK293 cells stably expressing epitope-tagged MOPr and arrestin-3 for the PathHunter assay. The procedure for membrane preparation was identical to that described above. For the assay itself, 10 μg of membrane protein was incubated in each well of a 96-well plate, diluted in a total volume of 250 μl of Hanks' buffered saline solution (HBSS; Invitrogen) containing 1 μM GDP, 0.5 mg of wheat germ agglutinin Scintillation Proximity Assay beads (GE Healthcare, Chalfont St. Giles, Buckinghamshire, UK), various concentrations of agonist and 300 pM [^{35}S]GTPγS (1 mCi/ml; PerkinElmer Life and Analytical Sciences, Waltham, MA). On each plate a concentration-response curve to DAMGO was constructed and the data for all other agonists normalized to that obtained for DAMGO. Reactions were allowed to proceed for 1 h before plates were centrifuged at 1500*g* for 2 min and scintillation was read on a TopCount scintillation counter (PerkinElmer Life and Analytical Sciences).

Arrestin Translocation Assay. HEK293 cells stably expressing arrestin-3 epitope-tagged with an EA moiety for the PathHunter

assay (DiscoveRx) were stably transfected with the MOPr:ProLink receptor construct. For assays, the cells were plated the day preceding the assay at ~10,000 cells/well in 20-μl volumes in a 384-well ViewPlate (PerkinElmer Life and Analytical Sciences). On the day of the assay, medium was removed and replaced with HBSS containing 0.1% bovine serum albumin and 20 mM HEPES, pH 7.4. Drugs were added in 5-μl volumes to the wells, and left to incubate for 2 h at 22°C. After incubation, 25 μl of proprietary Flash reagent mixed with lysis buffer was added to each well using a Minitrak liquid handling system (PerkinElmer), and luminescence was read after 3 min on a Leadseeker plate reader (GE Healthcare). Each concentration point had four replicates. Data were normalized relative to 30 μM alfentanil and a buffer control.

Ligand Binding Assay. Membranes were prepared as for the [^{35}S]GTPγS binding assay. For saturation binding experiments, [^{3}H]naloxone (1 mCi/ml; PerkinElmer Life and Analytical Sciences) was serially diluted 1:2 in HBSS, 20 mM HEPES, pH 7.4, from 60 nM down to 30 pM. Next, 10 μg of membrane protein was added to each well of a 96-well deep-well plate containing radioligand and HBSS and 20 mM HEPES, pH 7.4, with a total reaction volume of 500 μl. All radioligand binding experiments were performed in the presence of a physiologically relevant concentration of Na^+ (137 mM). Nonspecific binding was determined with 1 μM etorphine. Both total binding and nonspecific binding curves were performed in duplicate. To reach equilibrium, reactions were incubated at 22°C with agitation for 2 h after addition of radioligand. For competition binding experiments, competing ligands were prepared in concentration-response curves in HBSS and 20 mM HEPES, pH 7.4, in 96-well plates containing 10 μg of protein per well. Then 4 nM [^{3}H]naloxone was added to each well and binding reactions were left to incubate at 22°C for 2 h with agitation. Reaction plates were then harvested onto a 96-well filter plate using a Filtermate 96-well harvester (PerkinElmer Life and Analytical Sciences), with wash buffer (20 mM HEPES, pH 7.4), dried for 1 h and then read on a TopCount scintillation counter (PerkinElmer Life and Analytical Sciences), after addition of 40 μl of Microscint 20 scintillation fluid (PerkinElmer Life and Analytical Sciences) to each well.

FRET Experiments. Cells cotransfected with MOPr-YFP, arrestin-3-CFP, and GRK2 were plated out at ~40% confluence on poly-L-lysine–coated glass coverslips (25 mm diameter) in six-well plates 24 h before the experiments were performed. The coverslips were mounted on a Nikon Eclipse TE2000S inverted microscope (Nikon, Kingston, UK) using an "Attofluor" holder (Invitrogen, Leiden, The Netherlands), and the cells were continuously superfused with HBSS using a computer-assisted solenoid valve-controlled rapid superfusion device. Ligands were also applied using the same superfusion system. Cells were observed using an oil immersion 63× lens, a polychrome V (Till Photonics, Gräfelfing, Germany) for excitation, and a dual emission photometric system (Till Photonics). To minimize photobleaching, the illumination time was set to 10 to 50 ms applied with a frequency of 10 Hz. Fluorescence was measured at 535 ± 15 nm (F_{535}) and 480 ± 20 nm (F_{480}) (beam splitter dichroic long-pass, 505 nm; Chroma Technology, Rockingham, VT) upon excitation at 436 ± 10 nm (beam splitter dichroic long-pass, 460 nm; Chroma Technology). Signals detected by avalanche photodiodes were digitized using an analog/digital converter (Digidata 1322A; Molecular Devices, Sunnyvale, CA) and stored on PC using Axoscope 9.2 software (Molecular Devices). FRET was calculated as the ratio F_{YFP}/F_{CFP}.

Receptor Trafficking. Cell surface loss of MOPr was measured by enzyme-linked immunosorbent assay (ELISA) using a colorimetric alkaline phosphatase assay, as described previously (Bailey et al., 2003). In brief, HEK293 cells stably expressing T7-MOPr were first incubated with the primary antibody (anti-T7 monoclonal, 1:5000; Novagen Merck Chemicals, Nottingham, UK) for 60 min at 37°C to label surface MOPrs. Cells were then washed and incubated with

TABLE 1

Comparison of potency and maximum response of agonist-induced [^{35}S]GTPγS binding and arrestin-3 recruitment for 22 opioid agonists acting at MOPr in HEK293 cells

Agonists are positioned in the table according to potency in the [^{35}S]GTPγS binding assay, the most potent agonist (etorphine) being positioned at the top. Also shown are K_D values for the agonists as determined in [^{3}H]naloxone competition binding experiments. Max Response columns indicate maximum [^{35}S]GTPγS response for each agonist expressed relative to that obtained for DAMGO (taken as 1) and maximum arrestin-3 recruitment response for each agonist expressed relative to alfentanil (taken as 1), respectively. Apart from the exceptions noted, values represent mean ± S.E.M. of at least three independent experiments for each agonist.

Agonist	[^{35}S]GTPγS Binding		Arrestin-3 Recruitment		K_D
	EC_{50}	Max Response	EC_{50}	Max Response	
	nM		*nM*		*nM*
Etorphine	0.55 ± 0.16	0.92 ± 0.06	6.8 ± 1.0	1.22 ± 0.08	3.5 ± 0.3
Norbuprenorphine	1.7 ± 0.7	0.93 ± 0.02	84.6 ± 12.1	1.16 ± 0.09	24.6 ± 4.5
Met-enkephalin	7.7 ± 1.9	0.88 ± 0.06	939 ± 325	1.38 ± 0.16	281 ± 13
DAMGO	11.2 ± 1.93	1.04 ± 0.02	414 ± 90	1.24 ± 0.09	228 ± 74
Buprenorphine	14.5 ± 5.11	0.55 ± 0.04	—[a]	—	0.9 ± 0.1
Leu-enkephalin	30.9 ± 12.0	0.87 ± 0.05	5160 ± 1490	0.94 ± 0.10	744 ± 84
Levorphanol	33.1 ± 17.2	0.98 ± 0.11	265 ± 112	0.24 ± 0.03	23.2 ± 2.2
Fentanyl	56.8 ± 31.2	1.14 ± 0.11	210 ± 42	0.89 ± 0.13	158 ± 24
Pentazocine	77.9[b]	0.26[b]	—	—	149 ± 27
6MAM	73.3 ± 26.1	0.96 ± 0.03	1540 ± 700	0.45 ± 0.07	318 ± 86
M6G	81.0 ± 27.7	0.87 ± 0.06	1600 ± 370	0.27 ± 0.05	437 ± 227
Methadone	87.2 ± 42.2	1.18 ± 0.09	2110 ± 999	1.14 ± 0.16	552 ± 81
Alfentanil	90.3 ± 16.2	0.99 ± 0.01	638 ± 192	1.01 ± 0.16	866 ± 156
Morphine	97.5 ± 28.5	0.98 ± 0.03	322 ± 44	0.19 ± 0.03	250 ± 52
Endomorphin 2	138 ± 31	1.04 ± 0.04	311 ± 121	1.22 ± 0.01	283 ± 54
Endomorphin 1	183 ± 96	1.11 ± 0.11	226 ± 43	0.95 ± 0.04	281 ± 31
Normorphine	259 ± 165	1.11 ± 0.14	768 ± 165	0.52 ± 0.09	578 ± 141
Meptazinol	289[b]	0.38[b]	—	—	462 ± 71
Oxycodone	564 ± 195	0.95 ± 0.12	1460 ± 1290	0.18 ± 0.03	1550 ± 328
Meperidine	>10,000[c]	—	—	—	7110 ± 3300
Cyclazocine	>10,000[c]	—	—	—	17500 ± 725
Nalorphine	>10,000[c]	—	—	—	13.1 ± 0.6

6MAM, 6-monoacetylmorphine.

[a] It was not possible to determine values because maximum agonist response was not obtained or because of lack of significant response at highest agonist concentrations used.

[b] Values for these agonists determined from a curve fitted to the mean data, as it was not possible to obtain fits of individual curves.

[c] Estimation because maximum response was not obtained at the highest concentration of agonist used.

opioid agonists in Dulbecco's modified Eagle's medium for 30 min at 37°C. Cells were fixed in 3.7% formaldehyde and incubated with secondary antibody (goat anti-mouse conjugated with alkaline phosphatase, 1:1000; Sigma-Aldrich, Poole, Dorset, UK), a colorimetric alkaline phosphatase substrate (Bio-Rad Laboratories, Hemel Hempstead, Hertfordshire, UK) was then added, and samples were assayed at 405 nm with a microplate reader. The background was subtracted by simultaneous assay of HEK293 cells not expressing MOPr. Percentage cell surface receptor loss was calculated by normalizing data from each treatment group to corresponding control surface receptor levels determined from cells not exposed to opioid agonists. For each agonist, cell surface receptor loss was expressed as a percentage of that due to 10 μM DAMGO. All experiments were performed in triplicate.

Ser^{375} Phosphorylation. HEK293 cells stably transfected with T7-MOPr were plated onto poly-L-lysine–coated 60-mm dishes and grown to 90% confluence. After agonist treatment for 10 min, the cells were washed with ice-cold phosphate-buffered saline and harvested into ice-cold lysis buffer [50 mM Tris-HCl, pH 7.4, 1 mM EDTA, 120 mM NaCl, 40 mM glycerol-2-phosphate, 1% Triton X-100, 0.5 mM sodium orthovanadate, and the following proteinase inhibitors: 0.1 μM microcystin (Alexis Biochemicals, Exeter, UK), 4 mg/ml leupeptin, 4 mg/ml pepstatin A, 4 mg/ml antipain (all from Roche Diagnostics GmbH, Mannheim, Germany), and 4 mg/ml benzamidine (Sigma-Aldrich, Gillingham, Dorset, UK)]. The lysed cells were spun at 17,600*g* for 10 min at 4°C, and the pellet was discarded. The T7-tagged MOPr were then immunoprecipitated by incubation in an agitation system for 2 h at 5°C with 20 μl of protein Sepharose beads and 1 μl of anti-T7 monoclonal antibody (Novagen Merck Chemicals, Nottingham, UK). Immunocomplexes were precipitated, diluted in SDS sample buffer, and boiled at 95°C for 4 min. The immunoprecipitated MOPrs were then submitted to electrophoresis by SDS-polyacrylamide gel electrophoresis. After blotting, membranes were incubated with rabbit anti-phospho-Ser^{375} monoclonal antibody (1:1000 dilution; Cell Signaling Technology, Danvers, MA) for 1 h at room temperature, followed by detection using an enhanced chemiluminescence detection system.

Films exposed to Western blot membranes were scanned, and the amount of immunoreactive signal in each lane was quantified using Scion Image software (Scion Corporation, Frederick, MD). OD units of the immunoreactive bands were obtained. To reduce interexperimental variability, the relative immunoreactivity of the anti-phospho-Ser^{375}- MOPr band after different drug treatments was calculated as a percentage of the anti-phospho-Ser^{375}- MOPr band after treatment with 10 μM DAMGO obtained from a sample loaded on the same gel. The results are expressed as mean ± S.E.M. of three to seven independent experiments for each agonist.

Data Analysis and Statistics. The EC_{50} and maximum response values for [^{35}S]GTPγS binding and arrestin-3 translocation as shown in Table 1 were determined by fitting data from individual experiments to sigmoidal concentration-response curves with variable slope in Prism 4.0 (GraphPad Software, San Diego, CA), with mean and S.E.M. calculated using individual values from each experiment.

Analysis of concentration-response data for [^{35}S]GTPγS binding and arrestin-3 recruitment using the operational model of agonism (Black and Leff, 1983) was performed in Prism 4.0, fitting data for all agonists in a given assay simultaneously to the equation $Y = E_{max} \cdot T^n \cdot X^n/(K + X)^n + T^n \cdot X^n$. Here, T is tau ($\tau$) in the operational model of agonism; X is the molar concentration of agonist; K is the equilibrium dissociation constant (K_D) and was constrained to the K_D of the agonist as determined by competition binding; E_{max} is the theoretical maximum response of the system, and n represents a slope factor. To obtain values for the unknown variables E_{max}, τ, and n, data for all agonists were fit simultaneously to this equation by nonlinear regression. Both E_{max} and n were shared among all agonists in a given assay system, whereas τ was not constrained and allowed to vary for each agonist. E_{max} values were 1.05 for [^{35}S]GTPγS binding and 2.97 for arrestin-3 recruitment, whereas n values were 0.89 for [^{35}S]GTPγS binding and 1.76 for arrestin-3 translocation. The [^{35}S]GTPγS binding data were normalized to the maximum and minimum values evoked by DAMGO over a concentration range of 10 pM to 3 μM, as fitted to a concentration-response curve in Prism 4.0, whereas arrestin-3 recruitment data were normalized to the response evoked by 30 μM alfentanil.

The K_D values for agonists were determined by first fitting competition binding data normalized to buffer (total binding) and 1 μM etorphine (nonspecific binding) to a single site competition model in Prism 4.0. Mean and S.E.M. values for IC_{50} were then calculated from the individual values and were used to determine K_D values for the agonists using the transformation of Cheng and Prusoff (1973). The K_D value for [^{3}H]naloxone used in calculating K_D values were determined by fitting saturation binding data to a one-site binding model in Prism 4.0, with mean and S.E.M. again calculated from the individual values.

Correlation figures were produced by taking fitted values and corresponding standard errors from the respective analyses and obtaining r^2 values for the overall correlation in Prism 4.0. Correlations were considered to be statistically significant at $p < 0.05$.

Results

Agonist-Induced G Protein Activation. This was assessed using [^{35}S]GTPγS binding to membranes prepared from HEK293 cells stably expressing T7-tagged MOPr, full concentration-effect curves being obtained for 22 MOPr ligands. Curves for seven of the agonists (DAMGO, etorphine, norbuprenorphine, endomorphin 1, morphine, buprenorphine, and meptazinol) are shown in Fig. 1A, whereas the EC_{50} and maximum response values for all 22 of the agonists tested are shown in Table 1. Curves for all the agonists used are also plotted in Supplemental Fig. 1. The most potent agonist was etorphine (EC_{50}, 0.55 ± 0.16 nM), followed by norbuprenorphine (EC_{50}, 1.73 ± 0.70 nM). Most of the opioid drugs produced the same maximum response as DAMGO in this assay; only buprenorphine, pentazocine, meptazinol, and nalorphine produced a lower maximum response. A maximum response to cyclazocine could not be obtained at the highest concentration used (100 μM).

The agonist potency order for [^{35}S]GTPγS binding was the same when using membranes from HEK293 cells expressing the PathHunter system as when using membranes of HEK293 cells expressing T7-MOPr (Supplemental Fig. 2). This indicates that the ProLink moiety on the COOH terminus of MOPr required for the arrestin-3 translocation assay (see next section) does not interfere with G protein coupling.

Agonist-Induced Arrestin-3 Recruitment Using the PathHunter Assay. Arrestin translocation was studied using HEK293 cells stably expressing MOPr tagged with Prolink at the COOH terminus as well as arrestin-3 tagged at the COOH terminus with the EA moiety. In initial experiments, agonist-induced arrestin-3 recruitment induced by morphine and DAMGO increased with agonist incubation time, reaching a maximum by 2 h and declining somewhat at later times. As a consequence, an agonist incubation time of 2 h was chosen for all agonists. Curves for seven of the agonists are shown in Fig. 1B, whereas the EC_{50} and maximum response values for all the agonists tested are shown in Table 1. Curves for all the agonists used are also plotted in Supplemental Fig. 3. Etorphine was again the most potent agonist (EC_{50}, 6.8 ± 1.0 nM). In this assay, unlike in the [^{35}S]GTPγS assay, morphine, normorphine, 6-monoacetylmorphine, morphine-6-glucuronide (M6G) and levorphanol

had lower maximum responses than DAMGO. The agonists that had a lower maximum response in the [^{35}S]GTPγS assay (buprenorphine, pentazocine, meptazinol, and nalorphine) showed very little activity in the arrestin-3 assay. A maximum response to meperidine could not be obtained at the highest concentration used (100 μM).

Agonist-Induced Arrestin-3 Recruitment Monitored by FRET. The arrestin-3 translocation assay used above to construct full agonist concentration-effect curves was performed after agonist incubation for 2 h. Because most imaging assays of arrestin translocation normally take place after agonist addition for 30 min or less (Johnson et al., 2006), it was important to establish that the agonist-induced arrestin-3 interactions we had observed using the PathHunter assay system accurately reflected those that might be observed after short-term agonist application. To do this, we employed FRET to assess MOPr/arrestin-3 interactions in the minutes after agonist application. HEK293 cells were transiently transfected with MOPr-YFP, arrestin-3-CFP, and also GRK2 (the latter being necessary to see significant FRET in this assay); 48 h later, FRET was monitored for 5 min (8 min in the case of morphine) after the addition of saturating concentrations of some MOPr agonists; in each case, DAMGO (10 μM) was added after the first drug had been washed out (see Supplemental Fig. 4). Addition of DAMGO, endomorphin 1, endomorphin 2, and alfentanil each produced rapid increases in the FRET ratio (Fig. 2, A–D). Although etorphine also produced a marked increase in the FRET ratio, when the cells were washed, the FRET ratio did not decrease back toward baseline as it did with the other agonists but remained high such that no further response could be observed when DAMGO was added (Fig. 2E). Morphine produced a small increase in the FRET ratio compared with other agonists such as DAMGO (Fig. 2F), whereas neither buprenorphine nor pentazocine increased the FRET ratio when added to cells (Fig. 2, G and H). Indeed, DAMGO was unable to produce a FRET signal after application and washout of buprenorphine, an observation consistent with buprenorphine's reported partial agonist and long duration of action properties. Together, these results demonstrate that the acute effects of opioid ligands on arrestin recruitment reflect closely those obtained after longer agonist addition in the PathHunter assay.

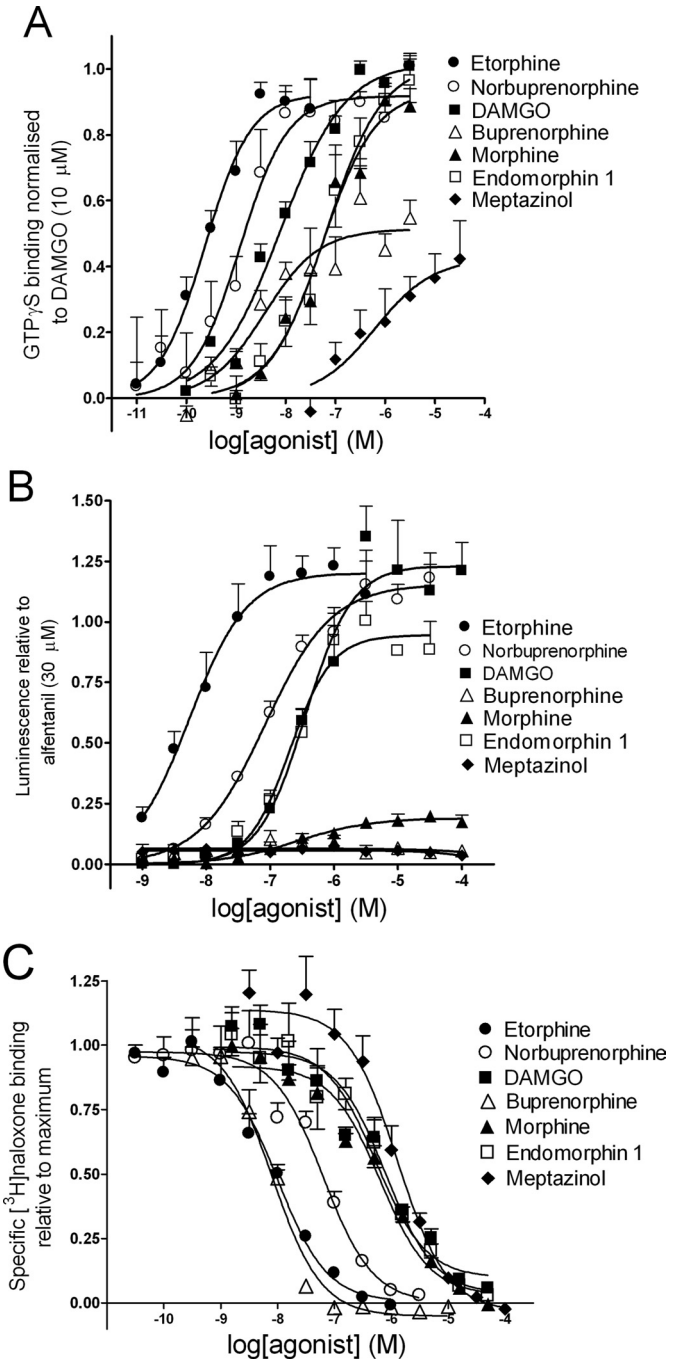

Fig. 1. MOPr agonist concentration-effect curves. Data were obtained in HEK293 cells for [^{35}S]GTPγS binding to membranes (A), arrestin-3 recruitment in intact cells using the PathHunter assay (B), and displacement of [^{3}H]naloxone from membranes (C). The same seven agonists are included on each of the three sets of axes, and in each graph, the mean data for each agonist have been fitted to a sigmoidal concentration response curve with variable slope. Values are means ± S.E.M. from three to six independent experiments.

Ligand Binding Experiments to Determine Ligand K_D Values at MOPr in the Presence of Na^+. To perform the operational analysis (see below), it was necessary to obtain K_D values for each agonist. This was done using radioligand displacement. All binding experiments were performed in HBSS buffer, which contains 137 mM Na^+. This concentration of Na^+ is the same as that to which the receptor is exposed in the [^{35}S]GTPγS and arrestin-3 assays as well as in the study of endogenous neuronal MOPr. Na^+ promotes binding of agonist ligands to a low-affinity binding site presumed to be uncoupled from G protein (Strange, 2008).

First, saturation binding of [^{3}H]naloxone to membranes of the HEK293 cells expressing T7-tagged MOPr was performed and the K_D of [^{3}H]naloxone binding determined to be 1.5 ± 0.3 nM and the B_{max} was 778 ± 6 fmol/mg protein (n = 3 independent experiments). Thereafter, ligand binding experiments were undertaken using 4 nM [^{3}H]naloxone. The MOPr ligands concentration-dependently displaced [^{3}H]naloxone binding from the membranes of HEK293 cells stably expressing T7-MOPr. Displacement curves for seven of the agonists are shown in Fig. 1C, and the K_D values for all the agonists are shown in Table 1. Curves for all the agonists used are plotted in Supplemental Fig. 5. Under the conditions used in the assay, buprenorphine and etorphine were the most potent displacers of [^{3}H]naloxone, whereas cyclazocine and meperidine were the weakest displacers.

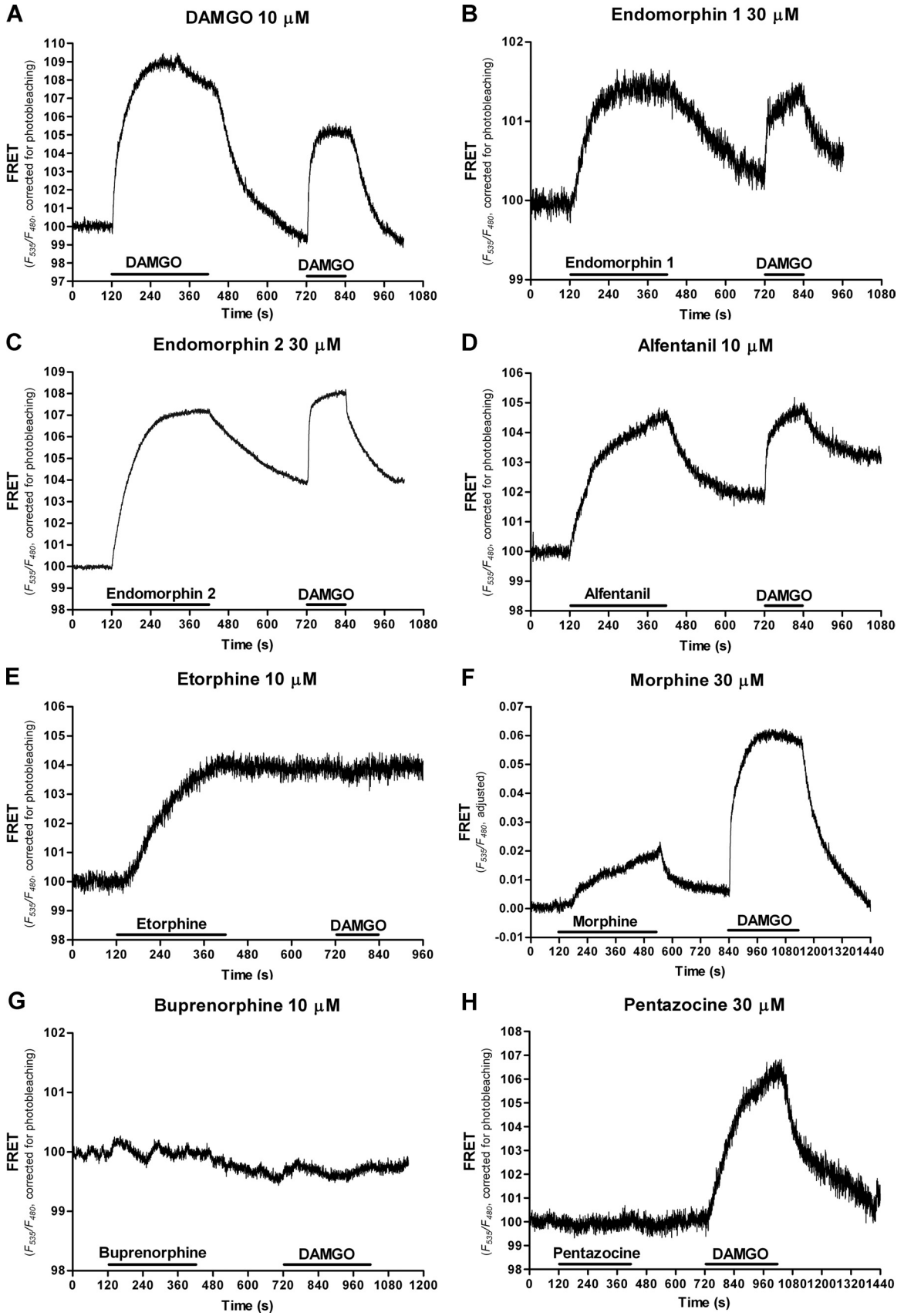

Fig. 2. Interaction of MOPr with arrestin-3 as measured by FRET. HEK293 cells were transiently transfected with rat MOPr-YFP, GRK2 and arrestin-3-CFP. To compare FRET responses between experiments, all drug applications (indicated by the horizontal bars) were followed by an application of 10 μM DAMGO. An increase in the FRET ratio (measured as F_{535}/F_{480}) reflects the interaction between MOPr-YFP and arrestin 3-CFP. Traces were filtered off-line with Axoscope 9.2. FRET traces were also corrected for photobleaching by converging the first 120 s to a one-phase

Saturation binding of [^{3}H]naloxone to membranes of the PathHunter HEK293 cells determined that the K_D of [^{3}H]naloxone binding was 1.2 ± 1.0 nM, and the B_{max} was 282 ± 46 fmol/mg protein (n = 3 independent experiments), indicating that the MOPr expression level in the PathHunter cells was 36% of that in the T7-MOPr cells.

Operational Analysis of Agonist Concentration-Effect Curves and Correlation of Operational Efficacy (τ) Values from [^{35}S]GTPγS and Arrestin-3 Recruitment Assays. Concentration-effect curves for agonists were subjected to operational analysis as described under *Materials and Methods*. Calculated τ values for each agonist in [^{35}S]GTPγS and arrestin-3 assays are shown in Table 2. In both assays, DAMGO and Met-enkephalin had the highest operational efficacy values. Somewhat surprisingly, the operational efficacy of etorphine for G protein activation was lower than those for six other agonists. Norbuprenorphine had much higher operational efficacy than buprenorphine for both G protein activation and arrestin-3 recruitment. Morphine, M6G, and oxycodone all had similar operational efficacy values for G protein activation and for arrestin-3 recruitment. The operational efficacy values of morphine for G protein activation and arrestin-3 recruitment were 18 and 27% of those for DAMGO, respectively. Furthermore, compared with most agonists, the endomorphins had relatively high values of operational efficacy for arrestin-3 recruitment compared with operational efficacy values for G protein activation. Finally, it should be noted that operational efficacy values of arrestin-3 recruitment for six agonists could not be determined (Table 2) because responses were not detected (see Fig. 2, G and H, and Supplemental Fig. 3), even though these compounds do have efficacy in other signaling assays (see Supplemental Fig. 1, also Selley et al., 1998; Borgland et al., 2003; Saidak et al., 2006).

A graph showing the correlation between operational efficacy values obtained in [^{35}S]GTPγS and arrestin-3 assays is shown in Fig. 3. Correlation of the data revealed a coefficient of 0.646 ($p < 0.05$), indicating a positive correlation between relative operational efficacy for G protein activation and arrestin-3 recruitment. Inspection of the correlation also indicates that endomorphins 1 and 2 appeared to be outliers (possibly also etorphine and fentanyl) as they displayed an apparent bias toward arrestin-3 recruitment.

It was not possible to present a log-log correlation graph (see Sykes et al., 2009) between operational efficacy values obtained in [^{35}S]GTPγS and arrestin-3 assays for all of the agonists tested because some of them had undetectable responses in the arrestin assay. Some of these agonists (e.g., buprenorphine and pentazocine) are clinically important opioids, and it was considered essential to include them on the correlation plot in Fig. 3. Nevertheless, a log-log correlation for the 16 agonists with quantifiable values of operational efficacy for arrestin recruitment is included in Supplemental Fig. 6.

Agonist-Induced Phosphorylation of Ser^{375} in MOPr. Ser^{375} in the COOH terminus tail of MOPr can be phosphorylated in an agonist-dependent fashion (Schulz et al., 2004). Using a commercially available anti-phospho-Ser^{375} antibody, we assessed the ability of a saturating concentration of 13 of the opioid agonists to induce phosphorylation of this residue (Fig. 4). In each case, the amount of agonist-induced phosphorylation is expressed as a percentage of that induced by a supramaximal concentration of DAMGO (10 μM). In general, the relative intrinsic activity (effect produced by a maximally effective concentration of the agonist relative to the response produced by a maximally effective concentration of an agonist that produced the greatest response) of the opioid agonists to induce phosphorylation of Ser^{375} in MOPr correlated well with the operational efficacy values for arrestin-3 translocation.

Agonist-Induced Cell Surface Loss of MOPr. An ELISA technique was employed to determine the effect of a receptor-saturating concentration of 21 of the opioid ligands on cell surface loss of MOPr, generally regarded as a reliable measure of agonist-induced GPCR internalization (Johnson et al., 2006). The results are shown in Fig. 5. In each case, the amount of agonist-induced internalization is expressed as a percentage of that induced by a maximally effective concentration of DAMGO (10 μM). The relative intrinsic activity of the opioid agonists to induce cell surface loss of MOPr correlated well with the operational efficacy values for arrestin-3 translocation.

Discussion

This study is the first to correlate the relative intrinsic efficacy of two MOPr signaling outputs for such a wide range of opioid ligands. It shows that, for these MOPr agonists, there is a strong positive correlation between the operational efficacies for G protein activation and arrestin-3 recruitment. Previous studies have provided very useful measures of relative intrinsic activity for MOPr agonists (Traynor and Nahorski, 1995; Yu et al., 1997; Kovoor et al., 1998; Zaki et al., 2000; Clark et al., 2006; Saidak et al., 2006), however this parameter is not able to differentiate full agonists in terms of efficacy and can be highly dependent upon receptor expression levels, so for these reasons, operational efficacy is a more useful measure. The operational model of agonism provides a measure of efficacy, termed operational efficacy, or τ (Black and Leff, 1983). Because τ is equal to R_T/K_e (where R_T is the receptor concentration in the tissue and K_e is the concentration of agonist-receptor complex that produces the half-maximal effect for that agonist in the tissue), then if measurements are made for a series of agonists acting at the same receptor population in a tissue, the tissue factors cancel out and the ratio of τ values become a measurement of relative intrinsic efficacy. Values of operational efficacy do not depend upon whether a particular agonist is a full or partial agonist in a tissue.

The GTPγS concentration-response data for the MOPr agonists revealed relative potency values largely in keeping with those reported in previous studies (Traynor and Nahorski, 1995; Emmerson et al., 1996; Selley et al., 1998), the majority of the agonists being full agonists and etorphine being the most potent agonist (Lee et al., 1999). On the other hand, a number of full agonists in the G protein assay were partial

exponential decay equation, with the exception of the morphine trace, which was manually adjusted by Axoscope 9.2. The absolute increase in FRET signal for each agonist varied between experiments, with a consequent increase in noise for smaller responses (e.g., B versus A). Data shown are representative of at least three independent experiments. An example of DAMGO-induced changes in F_{535}/F_{480} is shown in Supplemental Fig. 4.

agonists in the arrestin-3 recruitment assay, including morphine, normorphine, oxycodone, M6G, and 6-monoacetylmorphine. Furthermore, the agonist EC_{50} values obtained for arrestin-3 recruitment were all higher than the respective EC_{50} values for G protein activation. This can be explained by a combination of there being a greater receptor reserve for G protein activation than for arrestin-3 recruitment, and a greater level of MOPr expression in the HEK293 cells used for the [^{35}S]GTPγS binding compared with the cells used for the PathHunter assay.

To obtain K_D values for the agonists, competition binding experiments were undertaken in the same buffer as that used for the [^{35}S]GTPγS binding and arrestin-3 recruitment experiments, containing 137 mM Na^+. Agonist binding to some GPCRs is sensitive to the Na^+ concentration (Strange, 2008). Such an effect was observed for MOPr function many years ago (Pert et al., 1973) and explains why the K_D values we obtained in this study are higher than many of those previously published (e.g., Selley et al., 1998).

By fitting the data from the two functional assays to the operational model, τ values of operational efficacy for [^{35}S]GTPγS binding and arrestin-3 recruitment were obtained. Overall, there was a strong positive correlation between the τ values for [^{35}S]GTPγS binding and arrestin-3 recruitment ($r^2 = 0.646$). Previous investigations of the relationship between GPCR activation and regulatory processes such as phosphorylation, desensitization, and internalization have provided contrasting pictures. Although for some GPCRs there is a strong correlation between agonist-induced signaling and receptor phosphorylation/desensitization, for others there is a relatively poor correlation (e.g., Lewis et al., 1998). However, in most of these studies, relative intrinsic activity (relative maximum responses) has been used as the measure of efficacy rather than relative operational efficacy as in the present work.

TABLE 2

Calculated operational efficacy (τ) values for [^{35}S]GTPγS binding and arrestin-3 recruitment for twenty-two opioid agonists

Data were fitted to the operational model of pharmacological agonism as described in the Methods. Values are arranged in order of magnitude of the τ value for [^{35}S]GTPγS binding, with the highest (DAMGO) at the top. Each agonist concentration-effect curve was repeated at least three times; the τ values shown are the fitted values from operational analysis of all data ± S.E. of the fitted value.

Agonist	Operational Efficacy (τ)	
	[^{35}S]GTPγS	Arrestin-3 Recruitment
DAMGO	28.5 ± 1.1	0.82 ± 0.08
Met-enkephalin	22.0 ± 1.1	0.86 ± 0.20
Methadone	18.2 ± 0.9	0.67 ± 0.04
Leu-enkephalin	14.2 ± 0.9	0.56 ± 0.08
Norbuprenorphine	13.9 ± 0.8	0.71 ± 0.05
Fentanyl	12.3 ± 0.6	0.64 ± 0.08
Etorphine	11.3 ± 0.5	0.80 ± 0.09
Alfentanil	10.7 ± 0.6	0.76 ± 0.06
Normorphine	8.8 ± 0.4	0.44 ± 0.06
6MAM	6.6 ± 0.3	0.36 ± 0.03
Endomorphin 1	6.2 ± 0.2	0.71 ± 0.05
M6G	5.2 ± 0.2	0.25 ± 0.01
Morphine	5.2 ± 0.2	0.22 ± 0.01
Oxycodone	5.1 ± 0.2	0.23 ± 0.01
Endomorphin 2	5.1 ± 0.2	0.84 ± 0.08
Levorphanol	3.7 ± 0.1	0.21 ± 0.01
Buprenorphine	0.6 ± 0.1	—[a]
Meptazinol	0.5 ± 0.1	—
Pentazocine	0.3 ± 0.1	—
Meperidine	—	—
Cyclazocine	—	—
Nalorphine	—	—

[a] It was not possible to determine τ values because either a maximum response to the agonist could not be obtained at the highest concentration of agonist used, the maximum response produced by the agonist was too small, or a response was undetectable.

With regard to MOPr, a good correlation between receptor activation and internalization for a small series of agonists was reported (Zaki et al., 2000), whereas other studies indicated a poor correlation between MOPr activation and desensitization (Yu et al., 1997, Whistler et al., 1999). However in these latter two studies, in which the readout for MOPr function involved activation of G protein-gated K^+ channels (GIRK), interpretation of the results may have been confused by the use of methadone, which can directly inhibit GIRKs (Rodriguez-Martin et al., 2008). In the current study, because GIRK activation was not used as a signaling output, then the inclusion of methadone in the analysis is not problematic.

In a detailed study (Borgland et al., 2003), the relative intrinsic efficacy of four MOPr agonists for three functional readouts (Ca^{2+} current inhibition, desensitization of Ca^{2+} current inhibition, and MOPr internalization) in the same cell type was quantified. Although a good correlation between MOPr activation and desensitization was reported, there was a poor correlation between MOPr activation and internalization by the agonists, principally because of the low intrinsic efficacy of morphine to induce MOPr internalization compared with its ability to inhibit Ca^{2+} current and promote desensitization of Ca^{2+} current inhibition. In the present study, we have analyzed a much wider series of MOPr agonists and have quantified arrestin-3 recruitment rather than desensitization or internalization. Although it is reasonable to assume that arrestin-3 recruitment reflects the presence of the agonist-induced GRK/arrestin desensitization pathway, it should be borne in mind that for some agonists, MOPr regulation can be largely independent of GRKs/arrestins (Chu et al., 2008; Bailey et al., 2009a,b), whereas, on the other hand, nonvisual arrestins can be recruited to a GPCR to perform functions other than receptor regulation. In the present study, the operational efficacy value for morphine's ability to recruit arrestin-3 to MOPr was in line with the low operational efficacy value for G protein activation, as well as the limited ability of morphine to induce MOPr internalization and Ser^{375} phosphorylation. This suggests that the lack of MOPr internalization observed with morphine in many systems (Johnson et al., 2006) can be most simply explained by the agonist's low efficacy at MOPr.

Relative to other agonists studied, endomorphins 1 and 2 (and to a lesser degree etorphine and fentanyl) are biased toward arrestin-3 recruitment. This was somewhat unexpected, as there is no previous evidence to suggest that the endomorphins induce MOPr signaling or regulation distinct from that of other agonists such as DAMGO. Indeed, in some studies of MOPr signaling outputs, the endomorphins seem to be partial agonists (e.g., Saidak et al., 2006). One possibility is that different agonists stabilize distinct active conformations of MOPr, which consequently have varying affinities for G protein and GRK/arrestins. This phenomenon, termed functional selectivity (Urban et al., 2007), has now been observed with particular agonists at a number of different GPCRs (Sanchez-Blazquez et al., 2001). Whether or not the endomorphins can stabilize an active conformation of MOPr

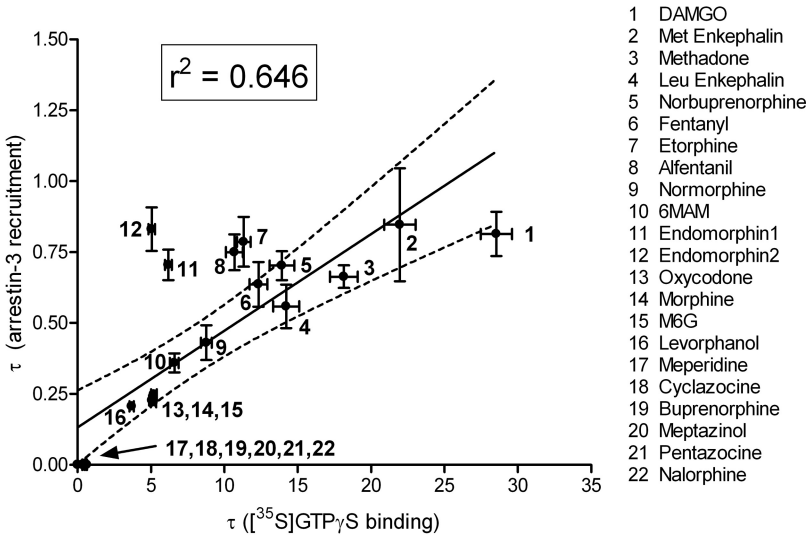

Fig. 3. Correlation of operational efficacy (τ) values for MOPr agonist-induced [^{35}S]GTPγS binding and arrestin-3 recruitment in HEK293 cells. Linear regression of data points revealed an r^2 value of 0.646 ($p < 0.05$); the dotted lines denote the 95% confidence intervals for the regression. The τ values shown are the fitted values from operational analysis of all data ± S.E. of the fitted value. 6MAM, 6-monoacetylmorphine.

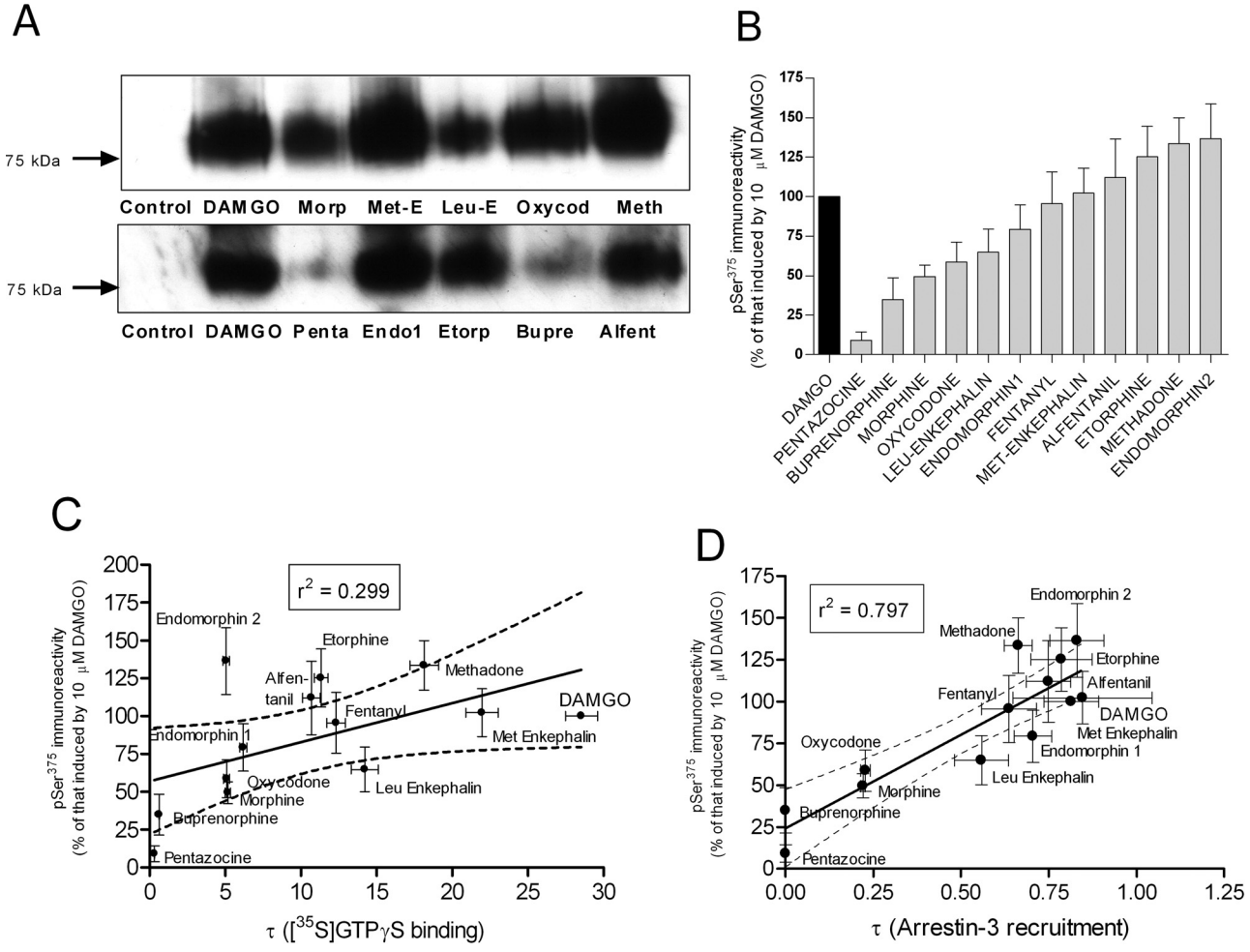

Fig. 4. Agonist-induced phosphorylation of Ser^{375} in the COOH terminus of MOPr detected with an anti-phospho-Ser^{375} antibody. A, examples of Western blots showing phosphorylation of Ser^{375} by receptor saturating concentrations of different MOPr agonists. B, phosphorylation of Ser^{375} induced by 13 MOPr agonists, normalized to that induced by DAMGO (10 μM). Values are means ± S.E.M. from at least three different experiments. The agonist concentration was 10 μM for etorphine, buprenorphine, met-enkephalin, leu-enkephalin, fentanyl, and alfentanil, and 30 μM for all other agonists. C, correlation of agonist relative intrinsic activity for Ser^{375} phosphorylation with operational efficacy (τ) values for [^{35}S]GTPγS binding. Linear regression of the data revealed an r^2 value of 0.299. Phosphorylation values are expressed as means ± S.E.M., whereas the τ values for [^{35}S]GTPγS binding are the fitted values from operational analysis of all data ± S.E. of the fitted values. D, correlation of agonist relative intrinsic activity for Ser^{375} phosphorylation with τ values for arrestin-3 recruitment. Linear regression of the data revealed an r^2 value of 0.797. MOPr phosphorylation values are expressed as means ± S.E.M., whereas τ values for arrestin-3 recruitment are the fitted values from operational analysis of all data ± S.E. of the fitted values. The dotted lines in C and D denote the 95% confidence intervals for the regression.

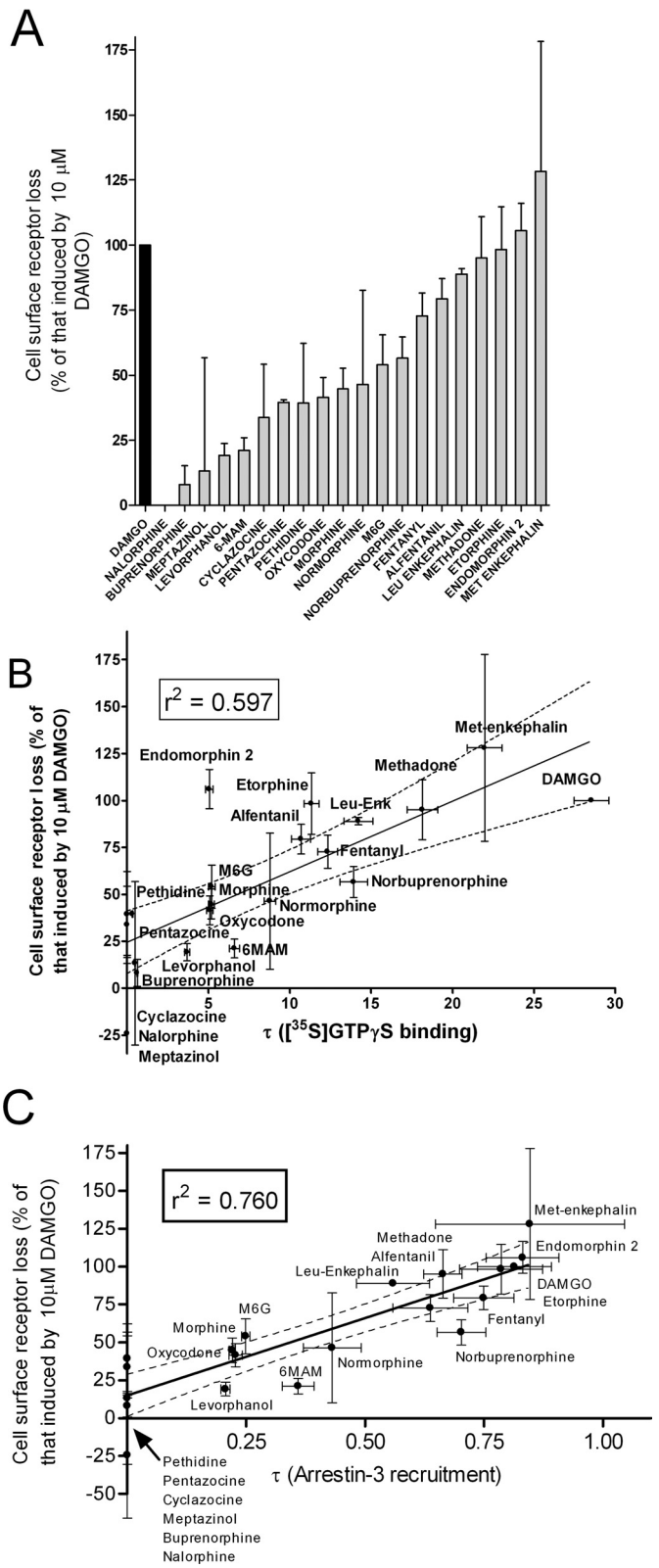

Fig. 5. Agonist-induced cell surface loss of MOPr. MOPr cell surface loss was measured by ELISA. A, cell surface loss of MOPr in response to saturating concentrations of agonist, normalized to that induced by DAMGO (10 μM). Agonist was applied for 30 min, which produced maximum cell surface loss of MOPr for DAMGO. Values are means ± S.E.M. from at least three different experiments. The agonist concentration was 10 μM for etorphine, met-enkephalin, leu-enkephalin, buprenorphine, fentanyl, alfentanil, and cyclazocine and 30 μM for the other agonists. B, correlation of agonist intrinsic activity for agonist-induced cell surface loss with operational efficacy (τ) values for [35S]GTPγS binding. Linear regression revealed an r^2 value of 0.597. Cell surface loss values are expressed as means ± S.E.M., whereas the τ values for [35S]GTPγS binding are the fitted values from operational analysis of all data ± S.E. of the fitted values. C, correlation of intrinsic activity for agonist-induced cell surface loss with operational efficacy (τ) values for arrestin-3 recruitment. Linear regression revealed an r^2 value of 0.739. Cell surface loss values are expressed as means ± S.E.M., whereas the τ values for arrestin-3 recruitment are the fitted values from operational analysis of all data ± S.E. of the fitted values. The dotted lines in B and C denote the 95% confidence intervals for the regression.

that is distinct from, for example, Met-Enkephalin or DAMGO, remains to be determined.

Apart from the effects of the endomorphins, another somewhat unexpected feature of the present data was that the operational efficacy of etorphine for G protein activation was only around half that for Met-Enkephalin or DAMGO. It is noteworthy that preliminary recordings of MOPr agonist-induced K^+ channel activation in locus ceruleus neurons contained in slices of rat brainstem also indicate that etorphine has lower operational efficacy than DAMGO (J. Llorente, G. Henderson, and E. Kelly, unpublished observations). Etorphine is a full agonist at MOPr in all systems studied (Clark et al., 2006) and, because of its high potency, is generally considered to possess high efficacy at MOPr. However our results indicate that etorphine's high potency is due principally to a very high affinity for MOPr (Lee et al., 1999). This underlines the importance of obtaining measures of relative intrinsic efficacy when comparing agonist efficacy.

Finally, in this study, we also assessed the ability of some agonists to induce either MOPr internalization or phosphorylation of Ser^{375} in the COOH terminus of MOPr. There was a good correlation between the intrinsic activity for agonist-induced Ser^{375} phosphorylation and operational efficacy values for arrestin-3 recruitment and also between the intrinsic activity for internalization and operational efficacy values for arrestin-3 recruitment. Because for most GPCRs, GRK-mediated phosphorylation is considered to be an important step in arrestin recruitment, and because arrestin binding to most GPCRs is important for efficient internalization (Kelly et al., 2008), then the high degree of correlation between these measures is not unexpected.

In conclusion, this study demonstrates that, apart from a handful of agonists that include the endomorphins, MOPr agonists display a good correlation between the operational efficacy for G protein activation and the operational efficacy for nonvisual arrestin recruitment. Future studies will be directed toward determining whether an enhanced interaction of arrestins with the endomorphin 1- or 2-occupied MOPr has particular functional consequences. Morphine's limited ability to induce MOPr internalization in most systems can be explained by its low efficacy for MOPr signaling. We have previously suggested that for morphine, desensitization and tolerance are mediated in large part by protein kinase C, whereas for DAMGO, an agonist of high operational efficacy, desensitization and tolerance are mediated by GRK (Johnson et al., 2006; Bailey et al., 2009b; Hull et al., 2010). It will be important to determine whether for the majority of MOPr agonists the mechanism of desensitization (PKC versus GRK/arrestin) is simply a function of efficacy for G protein activation.

References

Bailey CP, Couch D, Johnson E, Griffiths K, Kelly E, and Henderson G (2003) μ-Opioid receptor desensitization in mature rat neurons: lack of interaction between DAMGO and morphine. *J Neurosci* **23:**10515–10520.

Bailey CP and Connor M (2005) Opioids: cellular mechanisms of tolerance and physical dependence. *Curr Opin Pharmacol* **5:**60–68.

Bailey CP, Smith FL, Kelly E, Dewey WL, and Henderson G (2006) How important is protein kinase C in μ-opioid receptor desensitization and morphine tolerance? *Trends Pharmacol Sci* **27:**558–565.

Bailey CP, Llorente J, Gabra BH, Smith FL, Dewey WL, Kelly E, and Henderson G (2009a) Role of protein kinase C and μ-opioid receptor (MOPr) desensitization in tolerance to morphine in rat locus coeruleus neurons. *Eur J Neurosci* **29:**307–318.

Bailey CP, Oldfield S, Llorente J, Caunt CJ, Teschemacher AG, Roberts L, McArdle CA, Smith FL, Dewey WL, Kelly E, et al. (2009b) Role of PKCα and G-protein-coupled receptor kinase 2 in agonist-selective desensitization of μ-opioid receptors in mature brain neurones. *Br J Pharmacol* **158:**157–164.

Black JW and Leff P (1983) Operational models of pharmacological agonism. *Proc R Soc Lond B Biol Sci* **220:**141–162.

Borgland SL, Connor M, Osborne PB, Furness JB, and Christie MJ (2003) Opioid agonists have different efficacy profiles for G protein activation, rapid desensitization, and endocytosis of μ-opioid receptors. *J Biol Chem* **278:**18776–18784.

Cheng Y and Prusoff WH (1973) Relationship between the inhibition constant (K1) and the concentration of inhibitor which causes 50 per cent inhibition (I50) of an enzymatic reaction. *Biochem Pharmacol* **22:**3099–3108.

Christie MJ (2008) Cellular neuroadaptations to chronic opioids: tolerance, withdrawal and addiction. *Br J Pharmacol* **154:**384–396.

Christopoulos A and El-Fakahany EE (1999) Qualitative and quantitative assessment of relative agonist efficacy. *Biochem Pharmacol* **58:**735–748.

Chu J, Zheng H, Loh HH, and Law PY (2008) Morphine-induced μ-opioid receptor rapid desensitization is independent of receptor phosphorylation and β-arrestins. *Cell Signalling* **20:**1616–1624.

Clark MJ, Furman CA, Gilson TD, and Traynor JR (2006) Comparison of the relative efficacy and potency of μ-opioid agonists to activate $G\alpha_{i/o}$ proteins containing a pertussis toxin-insensitive mutation. *J Pharmacol Exp Ther* **317:**858–864.

Connor M, Osborne PB, and Christie MJ (2004) Mu-opioid receptor desensitization: is morphine different? *Br J Pharmacol* **143:**685–696.

Corbett AD, Henderson G, McKnight AT, and Paterson SJ (2006) 75 years of opioid research: the exciting but vain quest for the Holy Grail. *Br J Pharmacol* **147 (Suppl 1):**S153–S162.

Duttaroy A and Yoburn BC (1995) The effect of intrinsic efficacy on opioid tolerance. *Anesthesiology* **82:**1226–1236.

Emmerson PJ, Clark MJ, Mansour A, Akil H, Woods JH, and Medzihradsky F (1996) Characterization of opioid agonist efficacy in a C_6 glioma cell line expressing the μ opioid receptor. *J Pharmacol Exp Ther* **278:**1121–1127.

Furchgott RF and Bursztyn P (1967) Comparison of dissociation constants and of relative efficacies of selected agonists acting on parasympathetic receptors. *Ann NY Acad Sci* **144:**882–898.

Grecksch G, Bartzsch K, Widera A, Becker A, Höllt V, and Koch T (2006) Development of tolerance and sensitization to different opioid agonists in rats. *Psychopharmacology* **186:**177–184.

Hull LC, Llorente J, Gabra BH, Smith FL, Kelly E, Bailey C, Henderson G, and Dewey WL (2010) The effect of protein kinase C and G protein-coupled receptor kinase inhibition on tolerance induced by μ-opioid agonists of different efficacy. *J Pharmacol Exp Ther* **332:**1127–1135.

Johnson EA, Oldfield S, Braksator E, Gonzalez-Cuello A, Couch D, Hall KJ, Mundell SJ, Bailey CP, Kelly E, and Henderson G (2006) Agonist-selective mechanisms of μ-opioid receptor desensitization in human embryonic kidney 293 cells. *Mol Pharmacol* **70:**676–685.

Kelly E, Bailey CP, and Henderson G (2008) Agonist-selective mechanisms of GPCR desensitization. *Br J Pharmacol* **153:**S379–S388.

Koch T and Höllt V (2008) Role of receptor internalization in opioid tolerance and dependence. *Pharmacol Ther* **117:**199–206.

Kovoor A, Celver JP, Wu A, and Chavkin C (1998) Agonist-induced homologous desensitization of μ-opioid receptors mediated by G protein-coupled receptor kinases is dependent on agonist efficacy. *Mol Pharmacol* **54:**704–711.

Krasel C, Bünemann M, Lorenz K, and Lohse MJ (2005) β-Arrestin binding to the β_2-adrenergic receptor requires both receptor phosphorylation and receptor activation. *J Biol Chem* **280:**9528–9535.

Lee KO, Akil H, Woods JH, and Traynor JR (1999) Differential binding properties of oripavines at cloned μ- and δ-opioid receptors. *Eur J Pharmacol* **378:**323–330.

Lewis MM, Watts VJ, Lawler CP, Nichols DE, and Mailman RB (1998) Homologous desensitization of the D_{1A} dopamine receptor: efficacy in causing desensitization dissociates from both receptor occupancy and functional potency. *J Pharmacol Exp Ther* **286:**345–353.

Martini L and Whistler JL (2007) The role of μ opioid receptor desensitization and endocytosis in morphine tolerance and dependence. *Curr Opin Neurobiol* **17:**556–564.

Pert CB, Pasternak G, and Snyder SH (1973) Opiate agonists and antagonists discriminated by receptor binding in brain. *Science* **182:**1359–1361.

Rodriguez-Martin I, Braksator E, Bailey CP, Goodchild S, Marrion NV, Kelly E, and Henderson G (2008) Methadone: does it really have low efficacy at μ-opioid receptors? *Neuroreport* **19:**589–593.

Saidak Z, Blake-Palmer K, Hay DL, Northup JK, and Glass M (2006) Differential activation of G proteins by μ-opioid receptor agonists. *Br J Pharmacol* **147:**671–680.

Sánchez-Blázquez P, Gómez-Serranillos P, and Garzón J (2001) Agonists determine the pattern of G-protein activation in μ-opioid receptor-mediated supraspinal analgesia. *Brain Res Bull* **54:**229–235.

Schulz S, Mayer D, Pfeiffer M, Stumm R, Koch T, and Höllt V (2004) Morphine induces terminal μ-opioid receptor desensitization by sustained phosphorylation of serine-375. *EMBO J* **23:**3282–3289.

Selley DE, Liu Q, and Childers SR (1998) Signal transduction correlates of μ opioid agonist intrinsic efficacy: receptor-stimulated [^{35}S]GTPγS binding in mMOR-CHO cells and rat thalamus. *J Pharmacol Exp Ther* **285:**496–505.

Strange PG (2008) Agonist binding, agonist affinity and agonist efficacy at G protein-coupled receptors. *Br J Pharmacol* **153:**1353–1363.

Sykes DA, Dowling MR, and Charlton SJ (2009) Exploring the mechanism of agonist efficacy: a relationship between efficacy and agonist dissociation rate at the muscarinic M_3 receptor. *Mol Pharmacol* **76:**543–551.

Traynor JR and Nahorski SR (1995) Modulation by μ-opioid agonists of guanosine-5′-*O*-(3-[^{35}S]thio)triphosphate binding to membranes from human neuroblastoma SH-SY5Y cells. *Mol Pharmacol* **47:**848–854.

Urban JD, Clarke WP, von Zastrow M, Nichols DE, Kobilka B, Weinstein H, Javitch JA, Roth BL, Christopoulos A, Sexton PM, et al. (2007) Functional selectivity and classical concepts of quantitative pharmacology. *J Pharmacol Exp Ther* **320:**1–13.

Whistler JL, Chuang HH, Chu P, Jan LY, and von Zastrow M (1999) Functional dissociation of μ opioid receptor signaling and endocytosis: implications for the biology of opiate tolerance and addiction. *Neuron* **23:**737–746.

Williams JT, Christie MJ, and Manzoni O (2001) Cellular and synaptic adaptations mediating opioid dependence. *Physiol Rev* **81:**299–343.

Yu Y, Zhang L, Yin X, Sun H, Uhl GR, and Wang JB (1997) μ Opioid receptor phosphorylation, desensitization, and ligand efficacy. *J Biol Chem* **272:**28869–28874.

Zaki PA, Keith DE Jr., Brine GA, Carroll FI, and Evans CJ (2000) Ligand-induced changes in surface μ-opioid receptor number: relationship to G protein activation? *J Pharmacol Exp Ther* **292:**1127–1134.

Address correspondence to: Dr. Eamonn Kelly, Department of Physiology and Pharmacology, School of Medical Sciences, University of Bristol, Bristol, BS8 1TD, UK. E-mail: e.kelly@bristol.ac.uk